INTERNATIONAL SOCIETY FOR SOIL MECHANICS AND GEOTECHNICAL ENGINEERING

SIMSG | ISSMGE

Probability Distribution of Falling Rock by Experiments and a Method to Assess Collision Hazard

N. Naito[1], I. Yishida[2], H. Nakase[3] and H. Tochigi[4]

ABSTRACT

Following the advancement of numerical analysis methods, such as the discrete element method, the behaviors of falling rocks due to slope failure can be estimated to some extent. The present study proposes a method for calculating the probability of a falling rock to collide with a specific structure based on the assumption that the distribution of the arrival positions of the falling rocks can be obtained from a numerical analysis. Because information about the intensity of a collision is just as important as its probability, the present study considers that the intensity of the impact is a factor of the residual distance and assesses the relationship between this residual distance and the exceedance probability. The residual distance denotes the additional travel of a falling rock that does not hit a structure and represents the amount related to the impact velocity when the rock does hit.

Introduction

When an earthquake occurs, slope failure may occur, thereby affecting the neighboring facilities. Appropriately assessing the effects of slope failure and establishing measures against slope failure are important tasks, and many studies have been performed using these tasks. When a slope exists near a nuclear power plant, an important structure, the stability of the slope during an earthquake is an important assessment item. It is important to verify a slope's safety against basic earthquake ground motion and assess the damage caused by slope failure or falling rocks, which are assumed to occur during an earthquake, by estimating the distribution of falling rocks due to slope failure. To understand total probability for assessing the collision hazard of rocks against a structure following slope failure and falling rocks when an earthquake occurs, the earthquake hazard, slope failure, falling rocks, and conditional probability used in the present study must be comprehensively assessed. The present study proposes a method to assess the conditional probability of damage caused by slope failure or falling rocks.

Assessments of the effects of slope failure and falling rocks vary considerably; thus, it is difficult to quantitatively assess the effects of slope failure and falling rocks on structures by performing a numerical calculation. Therefore, an assessment method that can account for the variance is

[1] Graduate Student in the Doctoral Course_Naoto NAITO, Civil Engineering and Industrial Management Engineering, Nagoya Institute of Technology, Gokiso-cho, Showa-ku, Nagoya, Aichi 466-8555, JAPAN, cjl18507@stn.nitech.ac.jp

[2] Professor _Ikumasa YOSHIDA, Department of Urban and Civil Engineering, Planning and Management, Tokyo City University, Tamadutumi 1-28-1, Setagaya-ku, Tokyo 158-8557, JAPAN, iyoshida@tcu.ac.jp

[3] Doctor of Philosophy in Engineering _Hitoshi NAKASE, Civil Engineering Operation Center, Tokyo Electric Power Services Co.,LTD, Shinonome 1-7-12, Koto-ku, Tokyo 135-0062, JAPAN, nakase@tepsco.co.jp

[4] Doctor of Philosophy in Engineering _Hitoshi TOCHIGI, Civil Engineering Research Laboratory Structural Engineering Sector, Central Reserch Institute of Electric power Industry, Wabiko 1646, Wabiko, Chiba 270-7794, JAPAN, tochigi@criepi.denken.or.jp

required. The arrival positions of falling rocks should be assessed using probability distributions. Assuming that the distribution of the arrival positions of falling rocks due to slope failure is given using the discrete element method (DEM), the present study assesses the probability distribution and attempts to establish a method to assess the probability of a falling rock to collide with a specific structure (collision probability). The present study examines slope failure as rock slope failure, in which multiple rocks fall simultaneously. Tochigi et al. performed two experiments in which rocks were dropped from the top of a slope: in one case, they were dropped individually, and in the other case, they were dropped simultaneously. The arrival positions of the dropped rocks were then plotted. Based on the results obtained from these experiments, the present study assesses the probable distribution of the arrival positions of the falling rocks and calculates the probability of them striking a particular structure. Because information about the intensity of a collision is just as important as its probability, the present study also attempts to create a collision hazard curve that expresses the intensity of the impact. In these experiments, only information regarding the distribution of the positions of the fallen rocks could be obtained. Therefore, the present study considers that the intensity of the impact is a factor of the residual distance and assesses the relationship between this residual distance and the exceedance probability. The residual distance denotes the additional travel of a falling rock that does not hit a structure and represents the amount related to the impact velocity when the rock does hit. The exceedance probability is the probability that at least one rock with an arbitrary residual distance collides with a structure.

Probability Distribution of the Arrival Positions of Falling Rocks Obtained by Performing Experiments

Overview of the Experiments by Tochigi

To examine the characteristics of the distribution of rocks scattered after slope failure, experiments were performed in which two sizes (20−30 mm and 40−80 mm) of rocks were dropped individually (one by one) and simultaneously (as a group). The rocks were selected based on Zingg's shape classification. Figure 1 shows an experiment in which rocks were dropped one by one (individual experiment) and an experiment in which rocks were dropped as a group (simultaneous experiment). The amounts of rocks dropped in the simultaneous experiments were 10 and 50 kg. In the individual experiment, 300 rocks were selected from rocks that were 20−30 mm and 40−80 mm, and the arrival position of each individual rock was recorded. After dropping a rock, the rock was removed from the flat plate and the next rock was dropped. The method of dropping a rock is as follows: (1) a rock was set just before the top of a slope at its center, as shown in Figure 1; (2) the long side of a rock was parallel to the inclination direction of the slope; and (3) a rock was pushed with a finger, little by little, until it dropped. Table 1 presents the four cases used in the present study.

Figure 2 shows the distribution of the arrival positions of the rocks in each of the four cases. As shown in this figure, no large difference was observed in the distribution of the arrival positions between cases 1a and 2a and between cases 1b and 2b. However, both rocks of 20−30 mm and of 40−80 mm moved longer distances in the individual experiment than in the simultaneous experiment. In the simultaneous experiment, the rocks were distributed mainly in a place just below the slope, and the rocks were partially piled up. The reasons for the differences in the

distributions of the arrival positions of the rocks are examined in the next section.
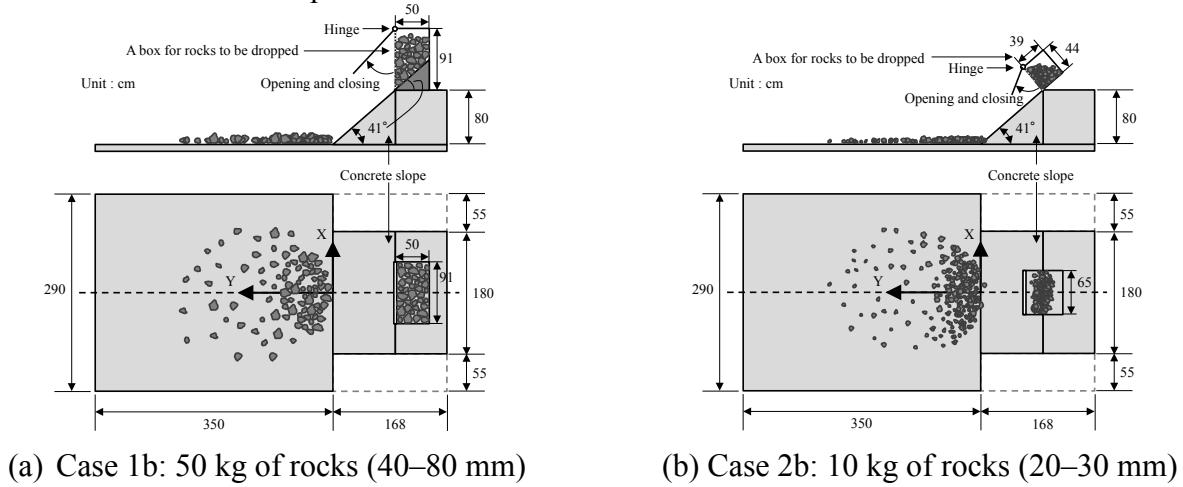

(a) Case 1b: 50 kg of rocks (40–80 mm)   (b) Case 2b: 10 kg of rocks (20–30 mm)

Figure 1. Outline of the experiments performed by Tochigi et al. at various sizes

Table 1. List of experiments

Case	1a	1b	2a	2b
Size of rocks	40-80 mm		20-30 mm	
Method of dropping rocks	Individual	Simultaneous (50 kg)	Individual	Simultaneous (10 kg)
Number of rocks	300	177	300	442

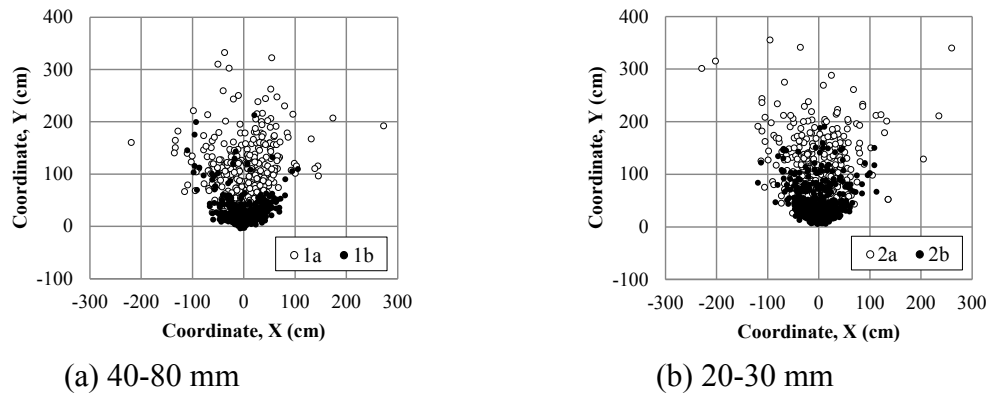(a) 40-80 mm   (b) 20-30 mm

Figure 2. Distribution of the arrival positions of falling rocks obtained in the experiments

Relationship between the Distribution of the Arrival Positions of the Rocks and the Collision Frequency

In this section, the reasons for the differences in the distributions of the arrival positions of the rocks between the two experiments are examined using DEM analysis. The present study reproduces the experiments performed by Tochigi et al. using the DEM analysis. Table 2 presents the parameters used in the analysis and a falling-rock model, in which five balls were sequentially connected with each other. A falling-rock model is a rigid body in which the relative

displacements of five balls are zero. In the normal contact model, if one ball rolls on a flat plate boundary layer, it will continue rolling. Therefore, it is necessary to model irregularities that are classified into bulk like rocks used in experiments. Meanwhile it is necessary to model the irregularities with as few balls as possible in order to prevent an increase in the calculation cost. The minimum number of balls that can reproduce the irregularity of the surface and construct a model of the bulk is five according to pre-calculation. The surfaces of the slope and the bottom were composed of a flat plate boundary layer. A contact model proposed by Cundall uses a spring, dashpot, non-tension divider, and slider. The parameters used for an interparticle contact model were also used for the contact model between particles and a plate in the present study.
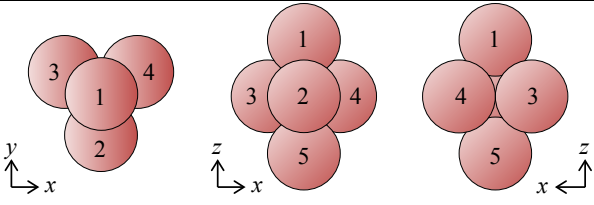
Table 2. Simulation parameters

Diameter of particle (m)	0.025	Falling-rock model	
Density (kg/m^3)	2600		
Spring coefficient (N/m)	2×10^{6}		
Viscous damping	0.258		
Frictional coefficient	0.566		

Figure 3 (a) shows the arrival position coordinates of case 1a, where falling-rock models were individually dropped, and those of case 1b, where falling-rock models were simultaneously dropped. The number of the models distributed on the foot of the slope was larger in case 1b than in case 1a, qualitatively reproducing the experimental results.

Figure 3 (b) shows the relationship of the average collision frequency per rock with the Y direction. The collision frequencies per rock at the top of the slope (Y = -1) and at the starting point of the flat section (Y = 0) were significantly higher in case 1b than in case 1a. This result likely occurs because the distance between rocks was small at the top of the slope immediately after collapse, making the average collision frequency high. Another reason is that a following rock collided with an already reached rock at the starting point of the flat section, further causing a high average collision frequency. When rocks were dropped as a group, they had difficulty reaching faraway places and were easily concentrated at the foot of the slope because the average collision frequency was high and energy was easily dispersed.
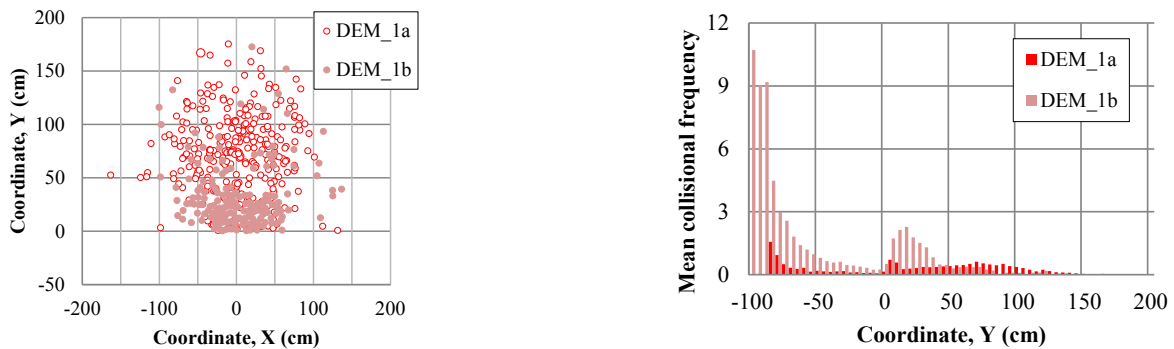
(a) Distribution of the arrival positions of the rocks (b) The average collision frequency per rock

Figure 3. DEM simulation results
Assessment of the Probability Distribution of the Arrival Positions of the Rocks

Models were created for the cumulative distribution probability of the arrival positions of the rocks in the X and Y directions. The method used to create a model for case 1a, where the rocks are individually dropped in the X direction, is described below. The arrival positions of the rocks are sorted in the order of smallest to largest coordinate value (x_i, $i = 1, …, n$). Here, n represents the rock number. Figure 4 shows the relationship between the coordinate value x_i and the standardization variable z_i in case 1a. In this figure, the vertical axis represents the coordinate value x_i, and the horizontal axis represents the standardization variable z_i that was obtained by the reverse calculation of the above probability.

$$P(x_i) = p_i = \frac{i}{n+1} \quad , \qquad z_i = \Phi^{-1}(p_i) \tag{1}$$

where Φ^{-1} represents the inverse function of the cumulative standard normal distribution. When the arrival positions of the rocks follow a normal distribution, the relationship between the coordinate value x_i and standardization variable z_i forms a straight line, the inclination of which represents the standard deviation, and the section of which represents the average. As shown in Figure 4, the relationship between the coordinate value x_i and standardization variable z_i forms an approximately straight line, so the model for case 1a can be created using a normal distribution. Similar to case 1a, Figure 3 shows the relationship between the coordinate value x_i and standardization variable z_i in the X direction for cases 1b, 2a, and 2b. Some rocks were not on a straight line in cases 1a and 2a, in which the rocks were dropped individually. In cases 1b and 2b, in which the rocks were dropped simultaneously, the rocks form an approximately straight line. The average arrival position was nearly zero in each case. The standard deviation was smaller in cases 1b and 2b than in cases 1a and 2a.

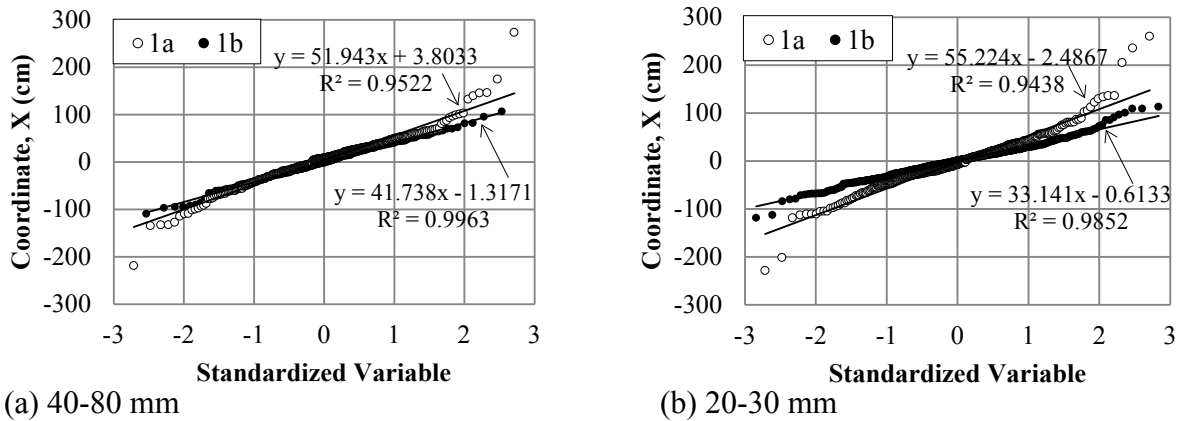(a) 40-80 mm   (b) 20-30 mm

Figure 4. Creation of models using a normal distribution of the arrival positions of falling rocks in the X direction
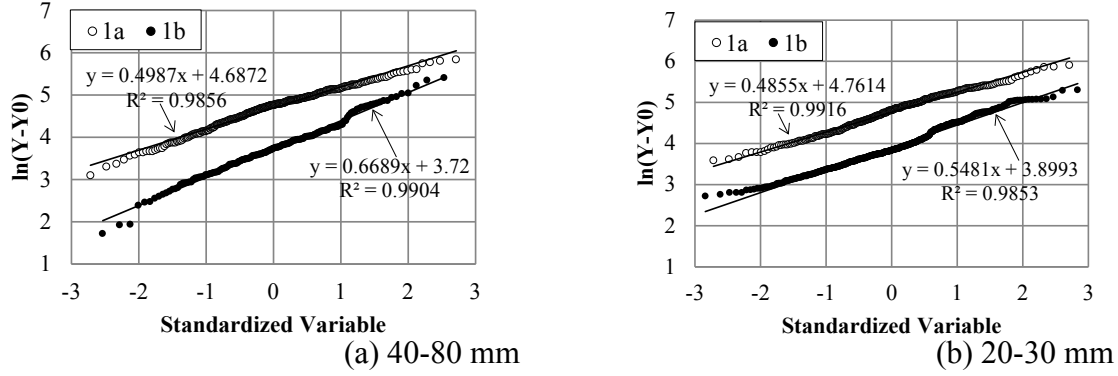
Figure 5. Creation of models using a logarithmic normal distribution of the arrival positions of falling rocks in the $\ln(Y-Y_0); Y_0 = 10$ cm

Next, the Y direction was handled as a logarithmic normal distribution because the rocks were concentrated at the foot of the slope and mainly distributed in the direction of the horizontal plane. In case 1b, although the foot of the slope was used as the origin of the Y coordinate, some rocks exhibited negative Y coordinate values; that is, these rocks were on the slope. These rocks could not be involved in the logarithmic normal distribution, so $Y-Y_0$ was applied to these rocks. Figure 5 shows the relationship between the coordinate value x_i and standardization variable z_i in the Y direction when $Y_0 = 10$ cm was applied to $\ln(Y-Y_0)$. As shown in this figure, the rocks formed an approximately straight line in each case, indicating that the model for each case can be created using a logarithmic normal distribution. The obtained averages and standard deviations are used to calculate the collision probability, as described below.

Methods to Assess the Collision Probability and Residual Distance Hazard Curve

Method of Calculating the Collision Probability

The collision probability and hazard curve were assessed based on the results obtained using the model described in Chapter 1. The collision probability in this study represents a conditional probability for when a slope failure or rockfall occurs. The collision probability is obtained by integrating the probability density distribution of the arrival position coordinates of a falling rock p(x, y). As shown in Figure 6 (a), the domain of integration was determined based on the assumption that falling rocks collided straight, with the specific structure in the center of the collapse region, and the region behind the specific structure was determined as the domain of integration. Although the entire region behind the specific structure should be integrated, the region with a certain area is actually sufficient for integration. As shown in this figure, segment d_a was set at the right and left sides to form a rectangular domain of integration, where the length of d_a is sufficiently large. Formula (3) expresses a two-dimensional integration problem, and several methods can be used to solve this problem. Because this problem was suitable for calculating the residual distance hazard, it was integrated using an interpolation function with quadrilateral elements (finite elements) as follows:

$$P_1 = \int_\Omega p(x, y)dxdy = \int_{-1}^{1}\int_{-1}^{1} p(r, s)|\mathbf{J}|drds \tag{2}$$

Coordinates *x* and *y* are a global coordinate system, and coordinates *r* and *s* are a local coordinate system. In the case where n rocks drop, the probability of at least one rock colliding against a specific structure (collision probability) can be calculated if these rocks are assumed to be independent of each other.
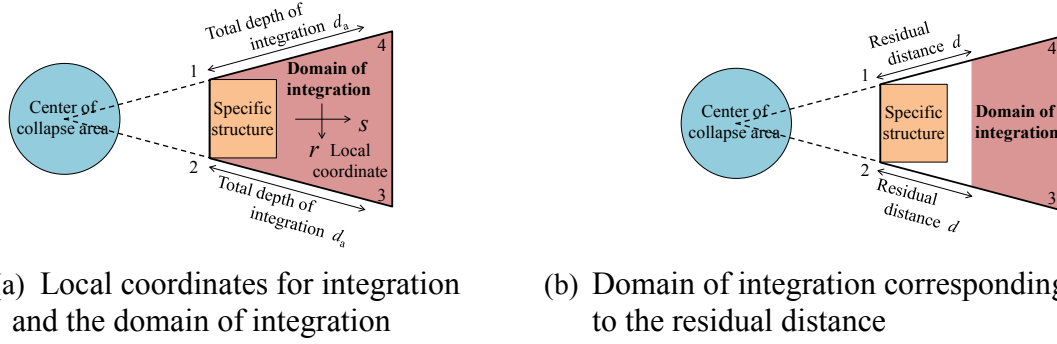

(a) Local coordinates for integration
and the domain of integration

(b) Domain of integration corresponding
to the residual distance

Figure 6. Domain of integration regarding the arrival position coordinates for calculating the collision probability

Method of Calculating the Residual Distance Hazard

The present study defines a curve that expresses the probability corresponding to the residual distance as a residual distance hazard. The exceedance probability corresponding to the residual distance *d* can be obtained by integrating the domain shown in Figure 6 (b). Because the local coordinate *s* represents the direction of a straight line from the center of the collapse region, the exceedance probability corresponding to the residual distance corresponding to the residual distance *d* is the value obtained by integrating the domain [-1 + 2*d*/*d*$_a$, 1] for local coordinate *s*. Therefore, the probability *P(d)* corresponding to the residual distance *d*, that is, the residual distance hazard curve, can be easily obtained.

$$P_1(d) = \int_{-1}^{1} \int_{-1+2d/da}^{1} p(r,s)|\mathbf{J}|drds \qquad (3)$$
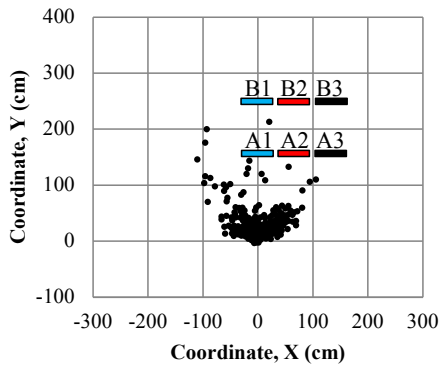
Examples of Assessing the Collision Probability and Residual Distance Hazard Curve

Based on the experimental results described in Chapter 1, the residual distance hazard curve is calculated as an example while assuming an appropriate structure. Regarding the probability density distribution *p(x, y)* of the arrival position coordinates of a falling rock necessary for Equation (5), a normal distribution is used for the *x* direction and a logarithmic normal distribution is used for the *y* direction, as described in Chapter 1. These two distributions are assumed to be independent of each other. In this case, the probability density distribution *p(x, y)* can be obtained using the following formula:

$$f(x,y) = \frac{1}{2\pi\sigma\varsigma y}\exp\left\{-\frac{(x-\mu)^2}{2\sigma^2} - \frac{(\ln(y-y_0)-\lambda)^2}{2\varsigma^2}\right\} \qquad (4)$$

where μ and σ represent the average and standard deviation in the X direction, respectively, and λ

and ζ represent the average and standard deviation when $Y_0 = 10$ cm was applied to $\ln(Y-Y_0)$, respectively. These averages and standard deviations are shown in Chapter 1. The coordinates of the collapse center were set as (0, -92 cm). The collapse center was required to determine the domain of integration for calculating the exceedance probability corresponding to the residual distance.

(a) Position of a structure assumed to calculate the collision probability
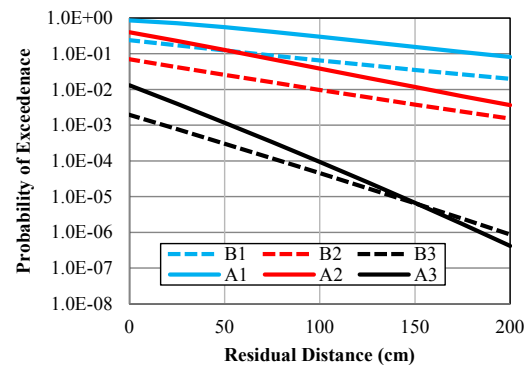
(b) Residual distance hazard curve corresponding to the location of a structure

Figure 7. Example of calculating the residual distance hazard curve

Figure 7 (a) shows specific structures A1, A2, A3, B1, B2, and B3. Each of these structures was expressed as a segment without considering the shape, and the region behind the segment was integrated to obtain the exceedance probability. Figure 7 (b) shows an example of calculating the residual distance hazard curve for case 1b. Figure 7 (b) shows the residual distance hazard for the probability of at least one rock colliding against a specific structure. The exceedance probability with a residual distance = 0 cm correspond to the collision probability. As shown in Figure 7 (b), the exceedance probability decreased as the residual distance increased (the collision became more severe). When A2 was compared with B1, the exceedance probability was slightly larger at A2 than at B1 because A2 was closer to the slope than B1. However, the exceedance probability with a residual distance > 60 cm was larger at B1 than at A2. Thus, the residual distance hazard curve can be assessed based on the positional relationship between the slope and a specific structure, and the exceedance probability corresponding to the residual distance can also be assessed.

Conclusion

The present study proposed a method to quantitatively assess the risk of slope failure to a structure based on the positional relationship between the slope and structure as the residual distance hazard. For this purpose, the present study created models based on the experimental results and used assessment examples. The present study used a method to assess the conditional probability when a slope failure or rockfall occurs. The model proposed in the present study can contribute to a practical method for assessing the probability and damage caused by a rock falling against a structure following slope failure triggered by an earthquake. Our future tasks are as follows:

(1) The first task is to create a new index for collision hazards. Although the residual distance is related to the impact force when a rock collides with a structure, this index is not always easy to use. We will create a model for the relationship between the impact velocity and residual distance, and we will calculate the impact velocity hazard using the created model.

(2) The second task is to develop a method to assess a three-dimensionally shaped landform. Currently, we are discussing how to develop the method. We will report these results in the future.

References

Atomic Energy Society of Japan: A standard for Procedure of Seismic Probabilistic Risk Assessment (PRA) for nuclear power plants, 2007.

Japan Nuclear Energy Safety Organization: Guideline for Design and Risk Evaluation against the Seismic Stability of the Ground Foundation and the Slope, *JNES-RE-2013-2037*, 2013.

Hitoshi Tochigi, Yasuki Ootori, Tadashi Kawai, Masato Nakajima and Makoto Ishimaru: Investigation of Influence Factor concerned with Traveling Distance-Development of Influence Area Prediction Method by Shaking Table Test of Slope Failure and Two Dimensional Distinct Element Analysis, *Civil Engineering Research Laboratory Rep.No.N08084*, 2009.

Hitoshi Tochigi: Investigation of Influence of Falling Rock Size and Shape on Traveling Distance due to Earthquake, *Civil Engineering Research Laboratory Rep.No.N09021*, 2010.

Ikumasa Yoshida, Keisuke Ohba and Makoto Ishimaru: Basic study on uncertainty related to failure phenomenon by MPS method or DEM, *Journal of Japan Society of Civil Engineering*, Ser.A2, Applied mechanics, Vol.**67**, No.2, I_365-I_374, 2011.

A.H-S. Ang, W.H. Tang (written), Manabu Ito, Hiroyuki Kameda (translation): Probability Concepts in Engineering Emphasis on Applications in Civil & Environmental Engineering, Maruzen, pp.260, 1977.

K.J.Bathe, E.L.Wilson (written), Fumio Kikuchi (translation): Numerical methods in finite element analysis, Kagaku Gijutsu Shuppan, 1979.

Zingg Th: Beitrag zur schotteranalysis, Schweiz. Min. Pentrol. Mitt., No.**15**, 1935.

Cundall, P. A. and O. D. L. Stack.: A Discrete Models for Granular Assemblies, *Geotechnique*, Vol.**29**, No.1, pp.47-65, 1979.